

“Adsorption, Desorption, and Displacement Kinetics of H₂O and CO₂ on Forsterite, Mg₂SiO₄(011)”

R. Scott Smith, Zhenjun Li, Zdenek Dohnálek, and Bruce D. Kay

*Fundamental and Computational Sciences Directorate, Pacific Northwest National Laboratory,
Richland, Washington 99352*

This supporting information file contains nine additional figures that are not necessary for the overall understanding of the scientific arguments presented in the main paper but may be of interest to some readers. Figure S1 and Figure S2 are XPS and XRD characterization spectra of the forsterite substrate, respectively. Figure S3 for and Figure S4 display representative sets of simulated TPD spectra and error analysis data are shown for CO₂ and H₂O, respectively. Figure S5 displays TPD desorption spectra for various amounts of CO₂ desorbing from 1 ML of H₂O deposited on forsterite. Figure S6 displays the $E(\theta)$ curve calculated using the inversion procedure for the saturation coverage spectrum in Figure S5. Figure S7 displays $E(\theta)$ curves calculated using the inversion procedure for two of the CO₂ TPD spectra in Figure 8. Figure S8 displays the H₂O TPD spectra for the corresponding CO₂ TPD spectra in Figure 8. The supporting information figures are referenced from the main text as Figure SX.

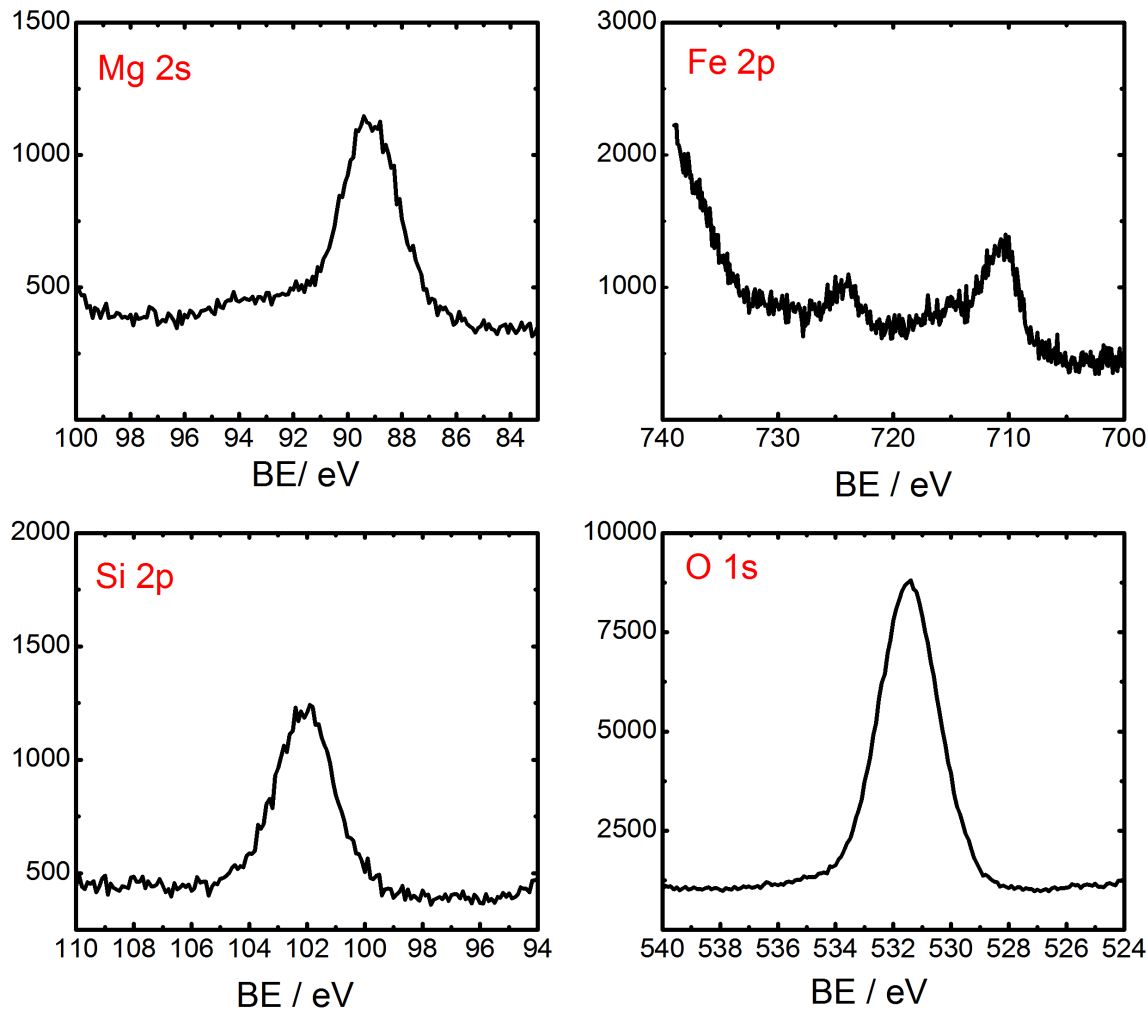


Figure S1 X-ray photoelectron (XPS) spectra of the natural forsterite substrate used in the present study. XPS measurements were acquired following sample cleaning (described in the main manuscript) using Mg K α radiation from a non-monochromated source. The hemispherical analyzer was a Physical Electronics Omni Focus III with variable apertures and a small-area lens. The results show that Si, O, Mg and Fe are all present of the substrate surface. Analysis of the sensitivity corrected intensities showed that Fe was \sim 10% of the total amount of Mg and Fe.

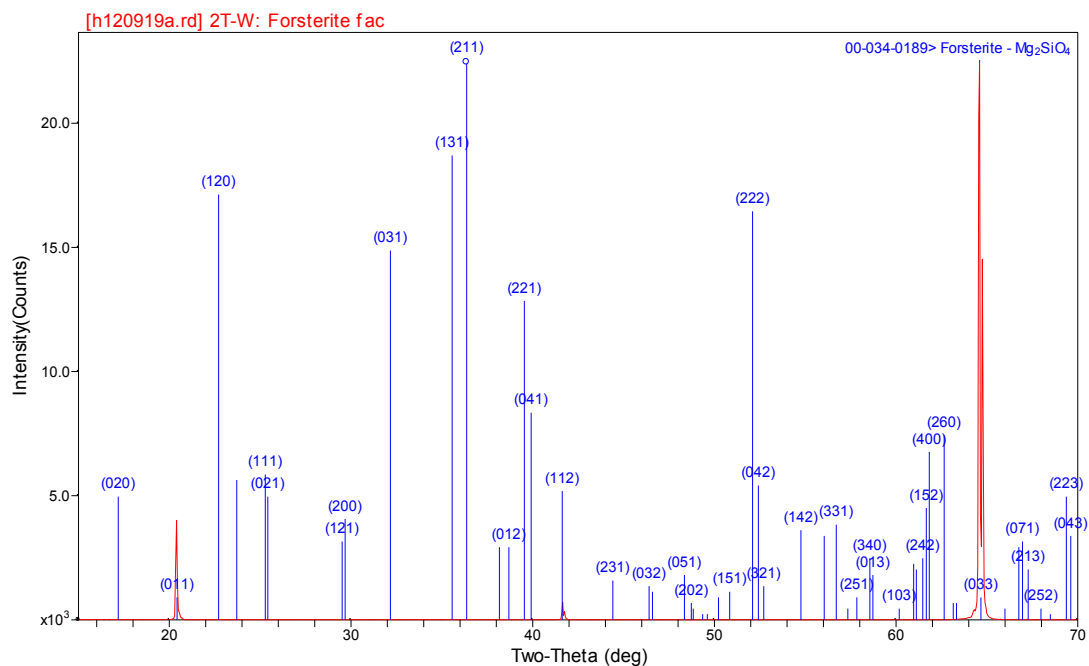


Figure S2 Xray-diffraction pattern for forsterite sample. The scan is a 2θ scan between 15° and 70° at a scan rate of $0.05^\circ/2s$. The reflection data are in red and the reference lines are in blue. The main reflections are at (011) and (033) which are consistent with the (011) surface.

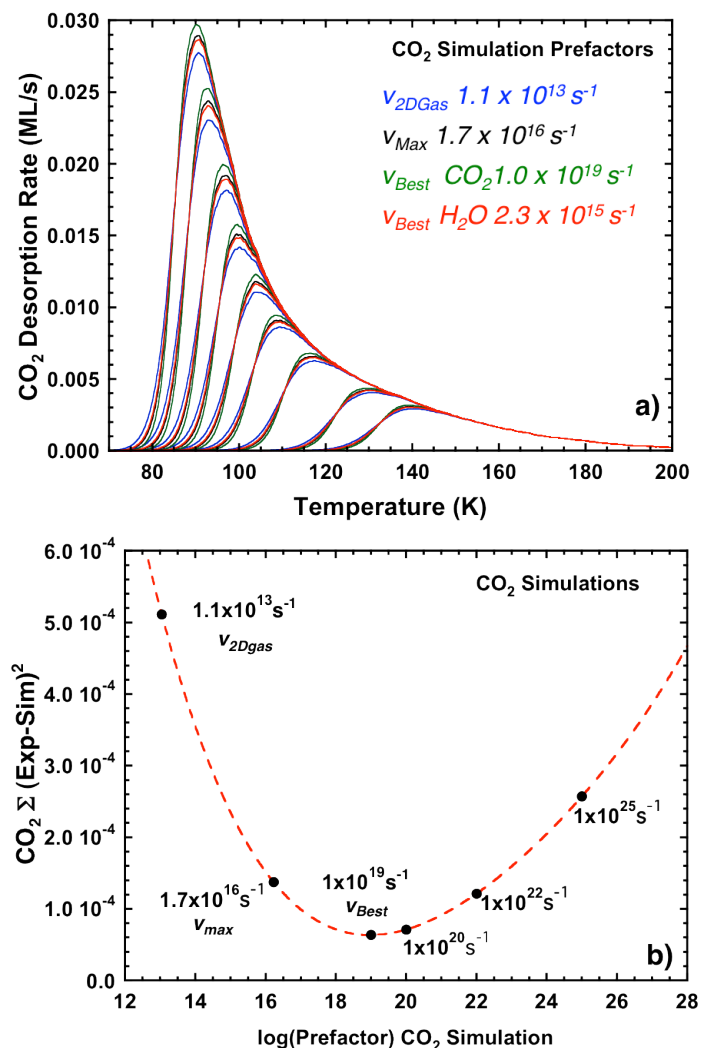


Figure S3 a) Sets of simulated CO₂ desorption spectra for various coverages (0.11, 0.16, 0.25, 0.33, 0.40, 0.48, 0.57, 0.69, and 0.80 ML) using the E(θ) curves obtained using various prefactors: $v_{2D gas} = 1.1 \times 10^{13} \text{ s}^{-1}$ (blue), $v_{Max} = 1.7 \times 10^{16} \text{ s}^{-1}$ (black), and $v_{Best} = 1.0 \times 10^{19} \text{ s}^{-1}$ (green). Also shown is a simulated set using and $v = 2.3 \times 10^{15} \text{ s}^{-1}$ which is the prefactor that yields a E(θ) curve that best fits the experimental H₂O TPD spectra. **b)** A plot of the sum of the χ^2 error between the experiment and simulation. The dashed line is a 4th-order polynomial fit to the error data used to determine the best prefactor, v_{best} , defined by the minimum. Note the 1 ML simulation is not shown since the simulations are identical for all prefactors.

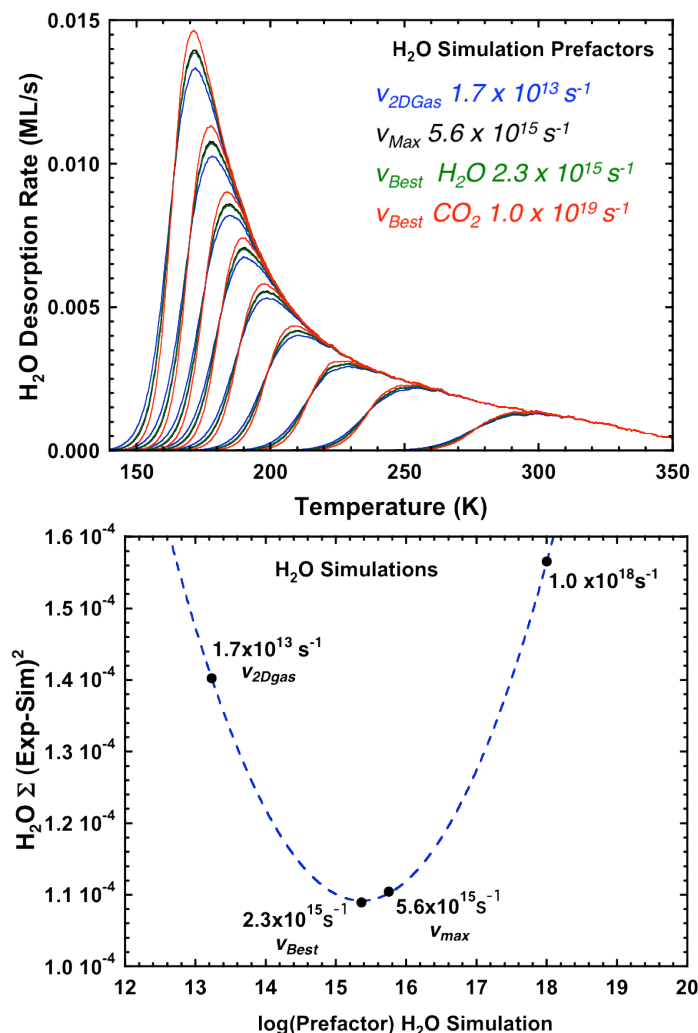


Figure S4 a) Sets of simulated H₂O desorption spectra for various coverages (0.07, 0.18, 0.24, 0.32, 0.40, 0.48, 0.55, 0.64, and 0.76 ML) using E(θ) curves obtained using various prefactors: $v_{2D gas} = 1.7 \times 10^{13} \text{ s}^{-1}$ (blue), $v_{Max} = 5.6 \times 10^{15} \text{ s}^{-1}$ (black), and $v_{Best} = 2.3 \times 10^{15} \text{ s}^{-1}$ (green). Also shown is a simulated set using $v = 1.0 \times 10^{19} \text{ s}^{-1}$ which is the prefactor that yields a E(θ) curve that best fits the experimental CO₂ TPD spectra. **b)** A plot of the sum of the χ^2 error between the experiment and simulation. The dashed line is a 2nd-order polynomial fit to the error data used to determine the best prefactor, v_{best} , defined by the minimum. Note the 1 ML simulation is not shown since the simulations are identical for all prefactors.

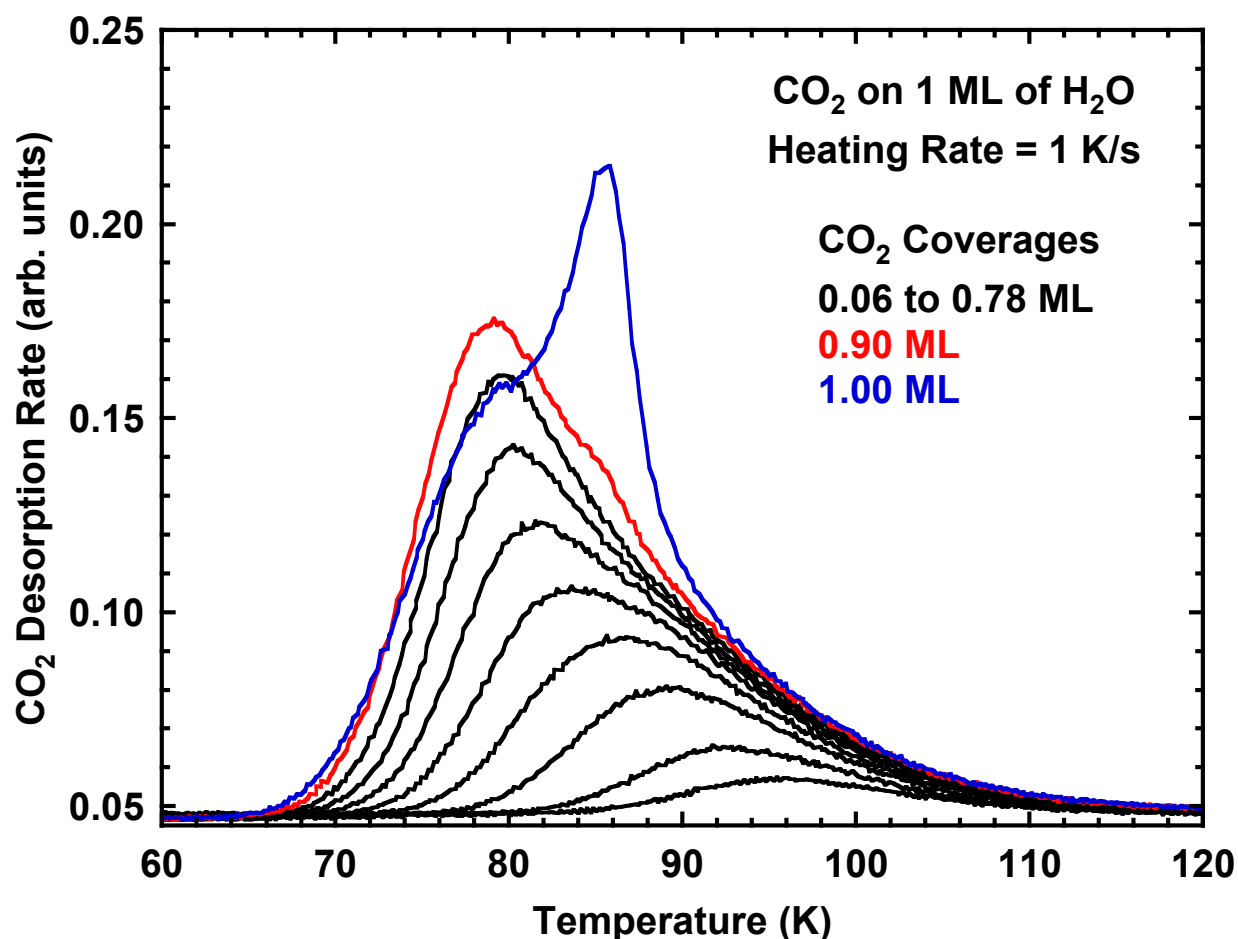


Figure S5 TPD desorption spectra for CO₂ from 1 ML of H₂O deposited on forsterite at 50 K and heated at 1 K/s. TPD spectra for CO₂ coverages of 0.06, 0.11, 0.22, 0.33, 0.44, 0.56, 0.67, and 0.78 ML (black curves), 0.90 ML (red curve), and 1.00 (blue curve). The 1.0 ML dose (blue curve) shows the onset of multilayer desorption. The shift of the multilayer peak to higher temperature indicates that the first layer of CO₂ on H₂O is metastable. A metastable CO₂ first layer is also apparent on forsterite in Figure 2 in the main text. In that figure the multilayer desorption leading edges cross under the monolayer desorption spectrum.

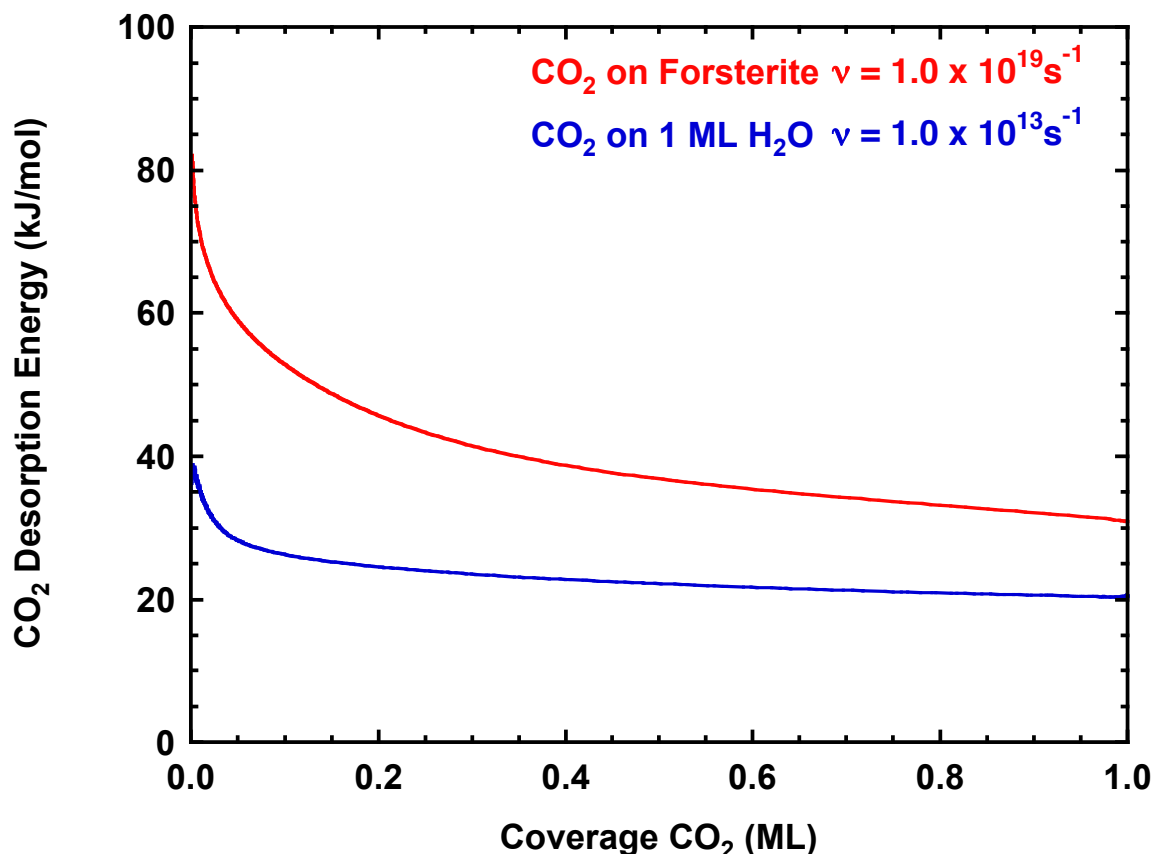


Figure S6 Coverage dependent binding energy curves for CO₂ on 1 ML H₂O on forsterite (blue line) obtained by inversion of the 0.9 ML spectra in Figure S5 using a prefactor of $1.0 \times 10^{13} \text{ s}^{-1}$. This curve saturates the H₂O surface and therefore for the inversion we redefine the 0.9 ML dose as being 1 ML. The red line is the coverage dependent binding energy curve for CO₂ on forsterite from Figure 3 and is redisplayed here for reference. The prefactor for this inversion was $\nu = 1.0 \times 10^{19} \text{ s}^{-1}$. A full simulation and error analysis procedure was not reasonable for the TPD data in Figure S5 because the trailing edges were not aligned. Instead we inverted all of the TPD spectra in Figure S5 with a series of prefactors and found that a value of $\nu = 1.0 \times 10^{13 \pm 3} \text{ s}^{-1}$ gave a set of $E(\theta)$ curves that were the most parallel (i.e. no upward or downward curvature). Despite the difference in binding energies, the desorption peak for 1 ML of CO₂ on either surface occurs at about the same temperature (see Figure 10 in the main text) due to the compensating nature of the prefactor and desorption energy.

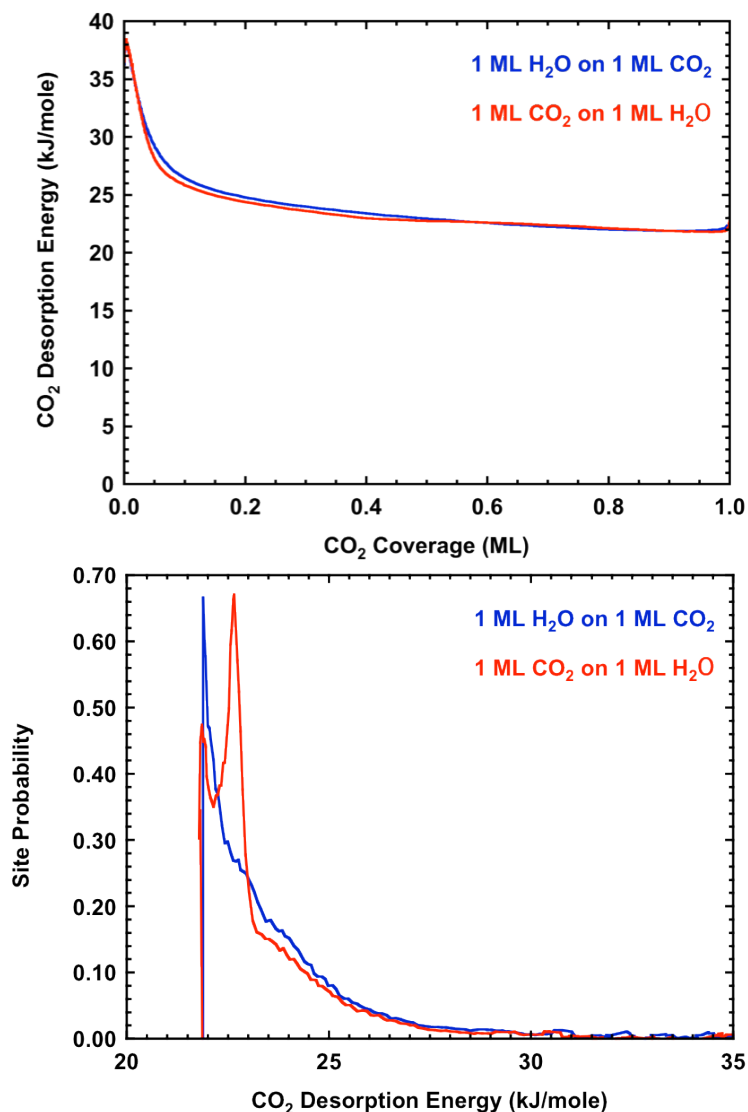


Figure S7 **a)** Inversion of two CO₂ desorption spectra from Figure 7 in the main text where 1 ML of CO₂ was dosed either before (blue) or after (red) 1 ML of H₂O. **b)** The desorption energy probability distribution, $P(E) = -d\theta/dE$ obtained by differentiating the $E(\theta)$ curves in a). The $E(\theta)$ and $P(E)$ curves are very similar confirming that the CO₂ desorption spectra are largely independent of the dose order. A prefactor of $1.0 \times 10^{13} \text{ s}^{-1}$ was used in the analysis because the desorption of CO₂ is most likely coming from the H₂O surface. The use of a different prefactor would simply shift the binding energies but the results for both inverted spectra would be nearly the same. These subtle differences in desorption energy ($\sim 1 \text{ kJ/mole}$) give rise to the small but readily discernable differences in the TPD spectra displayed in Figure 8.

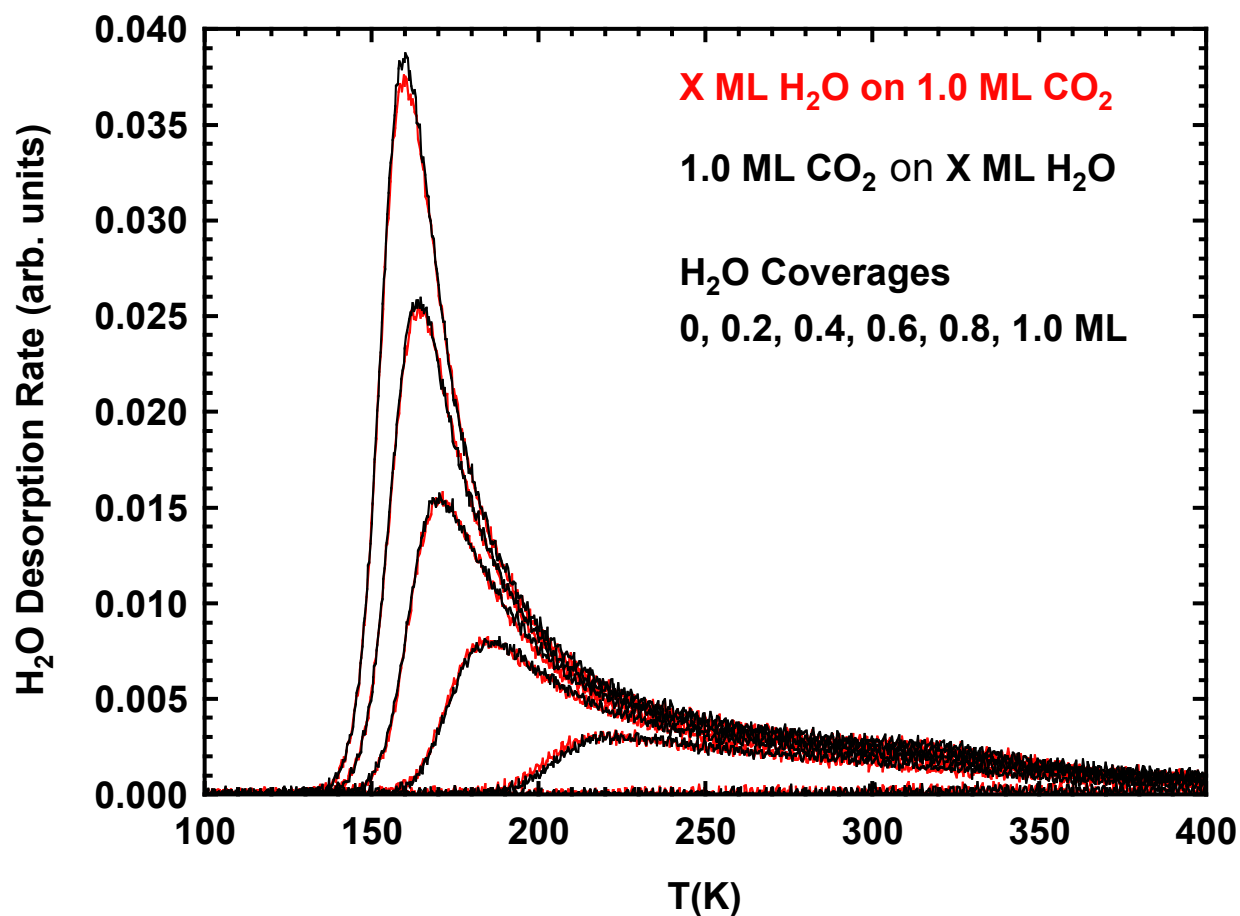


Figure S8 The corresponding H₂O TPD spectra from the experiments displayed in Figure 7 in the main text. In the experiments 1 ML of CO₂ is deposited before (red lines) and after (black lines) the deposition of various amounts of H₂O (0.0, 0.2, 0.4, 0.6, 0.8, and 1.0 ML). All depositions were at 50 K and the heating rate was 1 ML/s. The results show that the H₂O TPD spectra are independent of the dose order.